· Original article ·

BMSC-Exos affect inflammation and oxidative stress in DR rats by modulating the TLR4/NF-κB signaling pathway

Wang Qin[1,2], *Zeng Feng*[1], *Liu Wei*[2], *Huang Hao*[2], *Wang Haizhi*[1]

引用:王勤,曾凤,刘伟,等. 骨髓间充质干细胞来源外泌体通过调控 TLR4/NF-κB 信号通路影响 DR 大鼠炎症和氧化应激反应. 国际眼科杂志, 2026,26(8):1307-1315.

[1]Affiliated Qingyuan Hospital, Guangzhou Medical University; Qingyuan People's Hospital, Qingyuan 511518, Guangdong Province, China; [2]Zhuzhou Central Hospital; Zhuzhou Hospital Affiliated to Xiangya School of Medicine, Central South University, Zhuzhou 412007, Hunan Province, China

Correspondence to: Zeng Feng. Affiliated Qingyuan Hospital, Guangzhou Medical University; Qingyuan People's Hospital, Qingyuan 511518, Guangdong Province, China. Happy2008zhuzhu@163.com

Received: 2025-11-10 Accepted: 2026-05-15

骨髓间充质干细胞来源外泌体通过调控 TLR4/NF-κB 信号通路影响 DR 大鼠炎症和氧化应激反应

王 勤[1,2],曾 凤[1],刘 伟[2],黄 浩[2],王海治[1]

作者单位:[1](511518)中国广东省清远市,广州医科大学附属清远医院 清远市人民医院;[2](412007)中国湖南省株洲市,株洲市中心医院 中南大学湘雅医学院附属株洲医院

作者简介:王勤,毕业于广州医科大学,硕士研究生,住院医师,研究方向:眼底病。

通讯作者:曾凤,毕业于南华大学,硕士研究生,主任医师,教授,研究方向:眼底病. Happy2008zhuzhu@163.com

摘要

目的:研究骨髓间充质干细胞来源的外泌体(BMSC-Exos)对大鼠糖尿病视网膜病变(DR)的治疗作用,重点探讨其通过 TLR4/NF-κB 信号通路调节氧化应激和炎症反应的能力。

方法:由链脲佐菌素(STZ)诱导的糖尿病 SD 大鼠被随机分为 4 组:第 1 组[正常+磷酸盐缓冲液(PBS)]、第 2 组(正常+外泌体)、第 3 组(DR+PBS)以及第 4 组(DR+外泌体)。模型建立后第 8 wk,向玻璃体腔内注射 BMSC-Exos 或 PBS。第 16 wk 采集视网膜组织进行组织学分析[苏木精-伊红(HE)染色]、细胞凋亡检测(TUNEL 法),并评估氧化应激标志物[8-OHdG、超氧化物歧化酶(SOD)和谷胱甘肽(GSH)],并检测了炎症细胞因子[采用酶联免疫吸附测定(ELISA)检测白细胞介素-6(IL-6)和肿瘤坏死因子-α(TNF-α)]水平,以及分子谱分析[通过定量聚合酶链反应(qPCR)检测 *TLR4*, *NF-κB*, 和 *VEGF* 表达水平]。

结果:BMSC-Exos 显著抑制 DR 大鼠体内 TLR4/NF-κB 通路的激活($P<0.01$),同时伴有视网膜血管渗漏减少(伊文思蓝染色法,$P<0.001$)、细胞凋亡减少(TUNEL 检测,$P<0.05$)以及氧化应激反应减轻(SOD 和 GSH 升高、8-OHdG 水平降低,$P<0.05$)。炎症细胞因子(IL-6 和 TNF-α)水平显著下降($P<0.01$)。

结论:BMSC-Exos 通过抑制 TLR4/NF-κB 信号通路,减轻氧化应激、炎症反应及微血管功能障碍,从而缓解 DR。该研究为早期 DR 提供了新的治疗策略。

关键词:骨髓间充质干细胞;外泌体;TLR4/NF-κB 信号通路;氧化应激

Abstract

• AIM: To investigate the therapeutic effects of bone marrow mesenchymal stem cell-derived exosomes (BMSC-Exos) on diabetic retinopathy (DR) in rats, with a focus on their ability to modulate oxidative stress and inflammatory responses through the TLR4/NF-κB signaling pathway.

• METHODS: Streptozotocin (STZ)-induced diabetic Sprague-Dawley (SD) rats were randomly divided into four groups: Group 1 [normal+phosphate-buffered saline (PBS)], Group 2 (normal+Exos), Group 3 (DR+PBS), and Group 4 (DR+Exos). At the 8th week after modeling, BMSC-Exos or PBS were injected intravitreally. Retinal tissues were collected at the 16th week for histological analysis [hematoxylin and eosin (HE) staining], apoptosis detection (TUNEL). Oxidative stress markers [8-OHdG, superoxide dismutase (SOD), and glutathione (GSH)] were assessed, and inflammatory cytokines [enzyme-linked immunosorbent assay (ELISA) for interleukin (IL)-6 and tumor necrosis factor-alpha (TNF-α)], and molecular profiling [quantitative polymerase chain reaction (qPCR) for *TLR4*, *NF-κB*, and *VEGF*] were measured.

• RESULTS: The BMSC-Exos treatment significantly suppressed the activation of the TLR4/NF-κB pathway in DR rats ($P<0.01$), which was accompanied by reduced retinal vascular leakage (Evans blue assay, $P<0.001$), decreased apoptosis (TUNEL, $P<0.05$), and attenuated oxidative stress (elevated SOD and GSH, reduced 8-OHdG, $P<0.05$). The levels of inflammatory cytokines (IL-6 and TNF-α) were markedly decreased ($P<0.01$).

• CONCLUSION: BMSC-Exos alleviate DR by suppressing

the TLR4/NF-κB axis, thus reducing oxidative damage, inflammation, and microvascular dysfunction. This research offers a novel therapeutic approach for early-stage DR.

• KEYWORDS: bone marrow mesenchymal stem cells; exosomes; TLR4/NF-κB signaling pathway; oxidative stress
DOI:10.3980/j.issn.1672-5123.2026.8.02

Citation: Wang Q, Zeng F, Liu W, et al. BMSC-Exos affect inflammation and oxidative stress in DR rats by modulating the TLR4/NF-κB signaling pathway. Guoji Yanke Zazhi(Int Eye Sci), 2026,26(8):1307-1315.

INTRODUCTION

Diabetic retinopathy (DR) is a microvascular disease. Multiple interactions between retinal cells and neurons contribute to the development of DR[1]. The pathogenesis of DR is not entirely clear, but it may be related to various factors, including oxidative stress, inflammation, neovascularization, neurodegeneration, and neurovascular units. Among these factors, oxidative stress plays a particularly significant role[2]. The toll-like receptor 4/nuclear factor kappa-B(TLR4/NF-κB) signaling pathway is widely recognized as a pivotal mediator of oxidative stress, and elevated glucose levels can contribute to increased TLR4 expression. In individuals with diabetes, TLR4 not only is correlated with insulin resistance[3] but also triggers the downstream NF-κB[4], which then coordinates the control of chemokines and cytokines downstream. Furthermore, NF-κB signaling can be modulated in conjunction with reactive oxygen species (ROS), thereby promoting inflammation and apoptosis[5]. Studies have been conducted on therapeutic targets related to TLRs. By controlling TLR4/NF-κB signaling, microRNA-145 can reduce oxidative stress and inflammation in retinal endothelial cells caused by high hyperglycemia[6]. Exosomes have garnered significant attention across various fields, including oncology, cardiovascular research, and neurological studies. They have also been thoroughly investigated in the context of ocular diseases, notably DR. Current research on mesenchymal stem cell-derived exosomes has demonstrated that exosomes can successfully deliver miRNAs to the retina and treat DR[7]. Additionally, beyond non-coding RNAs, exosomes can directly deliver therapeutic macromolecules such as proteins, exerting direct therapeutic effects on target tissues and organs. In this paper, we demonstrate that bone marrow mesenchymal stem cell-derived exosomes (BMSC-Exos) may mitigate the progression of DR by targeting the TLR4/NF-κB pathway, which mediates oxidative and inflammatory damage. This suggests a potential for cell-free therapy in retinal protection.

MATERIALS AND METHODS

Ethical Approval An Ethics Committee approved the study and the approval number: LAEC-2023-002. The study was conducted in accordance with the ARVO Statement for the Use of Animals in Ophthalmic and Vision Research.

Main Materials and Instruments Male Sprague-Dawley rats (Guangdong Medical Laboratory Animal Center), streptozotocin (STZ) (Jizhi Biochemical Technology Co., Ltd., Shanghai, China), human bone marrow mesenchymal stem cells (Anbang Biotechnology Co., Ltd., Guangzhou, China), transmission electron microscopy (HITACHI, Japan), microsyringe (Shuopu Biotechnology Co., LTD., Guangzhou, China), CD63 antibody, FAS Eyeball Fixative, Iba-1 antibody, rat IL-6 enzyme-linked immunosorbent assay (ELISA) kit, terminal deoxynucleotidyl transferase dUTP Nick End Labeling (TUNEL) kit, reverse transcription kit, rat tumor necrosis factor-alpha (TNF-α) kit (Xavier Biotechnology Co., LTD., Wuhan, China), 8-hydroxy-2'-deoxyguanosine (8-OHdG) antibody (Santa CruzZ, USA), rat reduced glutathione (GSH) ELISA kit (Enzyme Immunity Industry Co., LTD., Jiangsu, China), and superoxide dismutase kit (Jiancheng Bioengineering Institute, Nanjing, China) were used.

Experimental Methods

Animal grouping, modeling, and vitreous exocytosis injection Healthy male 8-week-old (Sprague-Dawley rats, weighing between 200 and 250 g, were quarantined and isolated. They were then randomly divided into four groups: the normal+phosphate-buffered saline (PBS) (Group A), the normal+Exo (Group B), the DR+PBS (Group C), and the DR+Exo (Group D), with 12 rats in each group. No treatment was administered to the rats in Groups A and B. In contrast, Groups C and D were treated with STZ to create a model of DR. Following a 24-hour fast without access to water, the rats received an intraperitoneal injection of 60 mg/kg STZ citrate buffer. Food was reintroduced 2 h post-injection, and the following day, random glucose monitoring was conducted. If the concentration was lower than 16.7 mmol/L, STZ was injected intraperitoneally again. Rats with a glucose concentration higher than 16.7 mmol/L were considered diabetic. One week after establishing the model, the rats exhibited signs of diabetes, including polydipsia, polyphagia, polyuria, and weight loss. The rats were fed until week 8, at which point vitreous drug injections were administered. Rats in Groups A and C received 2 μL of PBS, while those in Groups B and D were injected with 2 μL of 1 μg/μL BMSC-Exos every two days for three consecutive injections. The rats were sacrificed at week 16, and subsequent experiments were conducted.

Exosome extraction and identification from BMSCs Human BMSCs were cultivated and cultured in serum-free media. Ultra-high-speed centrifugation was used to separate the exosomes from the cell supernatant, and the sample was subsequently centrifuged at 300×g for 10 min to remove the cells. The supernatant was centrifuged at 2000×g for 10 min to further remove the cells. The supernatant was further centrifuged at 10 000×g for 30 min to remove cellular debris. The exosomes were concentrated *via* an ultrafiltration membrane and centrifuged at 100 000×g for 70 min to collect

the exosomes. The supernatant was removed, and the mixed precipitate was resuspended in PBS and centrifuged at 100 000×g for 70 min. Exosomes were collected again, the supernatant was removed, and the mixed precipitate was resuspended in PBS. The samples were stored at −80 ℃ after filtration through a 0.22 − micron filter membrane. Transmission electron microscopy was used to observe the structure of exosomes, and Western blot was employed to detect the exosome signature protein CD63.

HE staining of rat retinal tissue sections Sixteen weeks following the establishment of the Sprague−Dawley model, the eyeballs were enucleated, washed in PBS, fixed in FAS eyeball fixative, embedded in paraffin, sectioned, and stained with hematoxylin and eosin (HE). The sections were dewaxed using xylene and ethanol, followed by a five − minute hematoxylin staining. After rinsing with distilled water, differentiation was performed using a 1% hydrochloric acid solution in ethanol. The sections were rinsed again in distilled water and counterstained with eosin for five minutes after being dehydrated in a graded series of alcohols for five minutes. The retinal tissue sections were then dehydrated with xylene, cleared, and mounted with neutral resin. The tissue morphology was observed under a microscope.

Evans blue dyeing At the eighth week post−vitreoretinal injection, rats from each group were randomly selected and administered a 45 mg/kg Evans blue staining solution *via* the tail vein, adjusted for their individual bodyweights. After 2 h, the rats' eyeballs were enucleated, and the retinal tissues were isolated. The retinas from each group were weighed and documented before being individually placed into light − shielded Eppendorf tubes containing 300 μL of formamide. These tubes were then incubated in a water bath at 60 ℃ for 24 h. The following day, the supernatant was subjected to centrifugation at 12 000 × g for 15 min and subsequently aspirated. The optical density (OD) values of each group were measured at 620 nm using a multifunctional enzyme marker. The residual concentration of Evans blue in the retinas of each group was determined from the standard curve.

TUNEL staining of rat retinas The TUNEL staining protocol was followed in accordance with the kit's instructions. Paraffin sections of rat retinal tissue were dewaxed using xylene and varying concentrations of ethanol, rinsed with distilled water, and subsequently treated with aproteinase K working solution at 37 ℃ for 22 min. The sections were washed with PBS and incubated with buffer for 10 min at room temperature. The TUNEL reaction mixture was then applied dropwise to cover the tissue in each section. Following incubation at 37 ℃ for 2 h, PBS was used to wash the wet box, and 4', 6 − Diamidino − 2' − phenylindole (DAPI) was employed to restain the cell nuclei. An antifluorescence quenching sealer was applied to seal the slices. The results were then examined using fluorescence microscopy.

Immunohistochemical staining of the rat retina Paraffin sections of rat retinal tissue were deparaffinized in water and endogenous peroxidase was removed through antigen retrieval with ethylenediaminetetraacetic acid (EDTA) (pH 9.0). Subsequently, a 3% hydrogen peroxide solution was applied. At room temperature, the samples were blocked with BSA after being incubated with an 8 − OHdG (1∶100) primary antibody overnight at 4 ℃. Following awash with PBS, the samples were incubated with a polyclonal horseradish peroxidase (HRP) − labeled goat anti − mouse secondary antibody at room temperature. Color development was achieved using diaminobenzidine (DAB), and hematoxylin was used to restain the cell nuclei. The sections were dehydrated and cleared by washing with running water. The results were examined under a microscope.

Immunofluorescence staining of the rat retina The paraffin sections of rat retinal tissue were deparaffinized using water and citric acid (pH 6). Antigen retrieval was followed by a 30−minute incubation with BSA at room temperature. The primary antibody against Iba − 1 (1∶500) was incubated overnight at 4 ℃. After a PBS wash, the sections were incubated with a fluorescent secondary antibody at room temperature under light−protective conditions. The cell nuclei were restained with DAPI. Following the reduction of autofluorescence, an anti−fluorescence quenching sealer was applied to seal the quenched tissues. The results were then photographed and observed under a fluorescence microscope.

Retinal tissue fluorescence quantitative PCR Total retinal RNA was extracted using Trizol, and a reverse transcription kit was utilized to convert the RNA into complementary DNA (cDNA). The resultant cDNA was amplified with SYBR Green qPCR Master Mix to assess the gene expression levels of vascular endothelial growth factor (VEGF), TLR4, and NF−κB. The data were analyzed using the 2−ΔΔCt method, and all experiments were conducted in triplicate. The sequences of the primers used are listed in Table 1.

Determination of IL − 6 and TNF − α concentrations in retinal tissue After centrifuging the retinal tissue homogenate to obtain the supernatant, we utilized an ELISA kit to measure the concentrations of TNF−α and IL−6 within the retinal tissue. The experiment was performed in accordance with the kit's instructions. OD of each well was measured at 450 nm, using a blank control well for zeroing. A standard curve was generated based on the concentrations and OD values of the standards, and the sample concentrations were determined using the equation derived from the standard curve. The experiment was repeated three times.

Table 1 Primer sequences

Target genes	Primer sequence 5'−3'
TLR−4	TGAGGACTGGGTGAGAAATGAGC
	CTGCCATGTTTGAGCAATCTCAT
NF−*κB*	GAGTCACGAAATCCAACGCAG
	CGTCATCACTCTTGGCACAATC
VEGF	AGGAGTACCCCGACGAGATAGA
	CACATCTGCTGTGCTGTAGGAA

Determination of the GSH concentration and SOD activity in retinal tissue After the retinal tissue homogenate was centrifuged to obtain the supernatant, a superoxide dismutase (SOD) assay kit and a reduced GSH kit were used to determine the SOD activity and GSH content, respectively, following the instructions provided. The OD values of each well were measured at 550 nm and 450 nm, after zeroing with blank control wells. The viability and concentration of the samples were calculated using the standard curve equation. The experiment was conducted in three iterations.

Statistical Analysis The statistical analysis was conducted using GraphPad Prism 8.0. One-way ANOVA was utilized to analyze differences among multiple groups, and the independent samples t-test was employed to compare two groups. Differences were considered statistically significant at $P<0.05$.

RESULTS

Characteristics of the BMSC-Exos After the exosomes were extracted using ultrahigh-speed centrifugation, their morphology was observed using transmission electron microscopy. The BMSC-Exos were found to be approximately 120 nm in diameter, exhibiting a disk-like, bilayer lipid membrane-encapsulated vesicle-like structure (Figure 1), consistent with the morphological and structural characteristics of exosomes. The Western blot results indicated that the BMSC-Exos extracted in this study expressed exosome-specific CD9 and CD63 proteins (Figure 2).

BMSC-Exos on Retinal Leakage in DR Rats Eight weeks following the intravitreal injection, the results of the Evans blue assay indicated a significant increase in retinal tissue leakage in Groups C and D compared to Groups A and B ($P<0.001$). Additionally, there was a significant reduction in leakage in Group D subsequent to the BMSC-Exo intervention ($P<0.001$, Figure 3).

BMSC-Exos on TLR4, NF-κB, and VEGF Expression in the Retinas of Rats with DR There was no significant difference in the gene expression of VEGF, TLR4, or NF-κB between Groups A and B ($P>0.05$). Compared with Group A, the expression level of VEGF in Group C was significantly greater after modeling ($P<0.01$), and after intravitreal injection of BMSC-Exos, the expression of VEGF in Group D was significantly lower ($P<0.01$, Figure 4C). Moreover, compared with Group A, *TLR4* and *NF-κB* gene expression levels were elevated in Group C after modeling ($P<0.01$), and after vitreous injection of BMSC-Exos, TLR4 and NF-κB expression levels were significantly decreased in Group D (both $P<0.01$, Figure 4A, 4B).

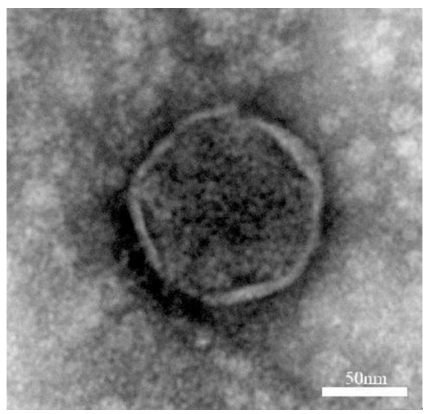

Figure 1 Exosome electron microscopy results.

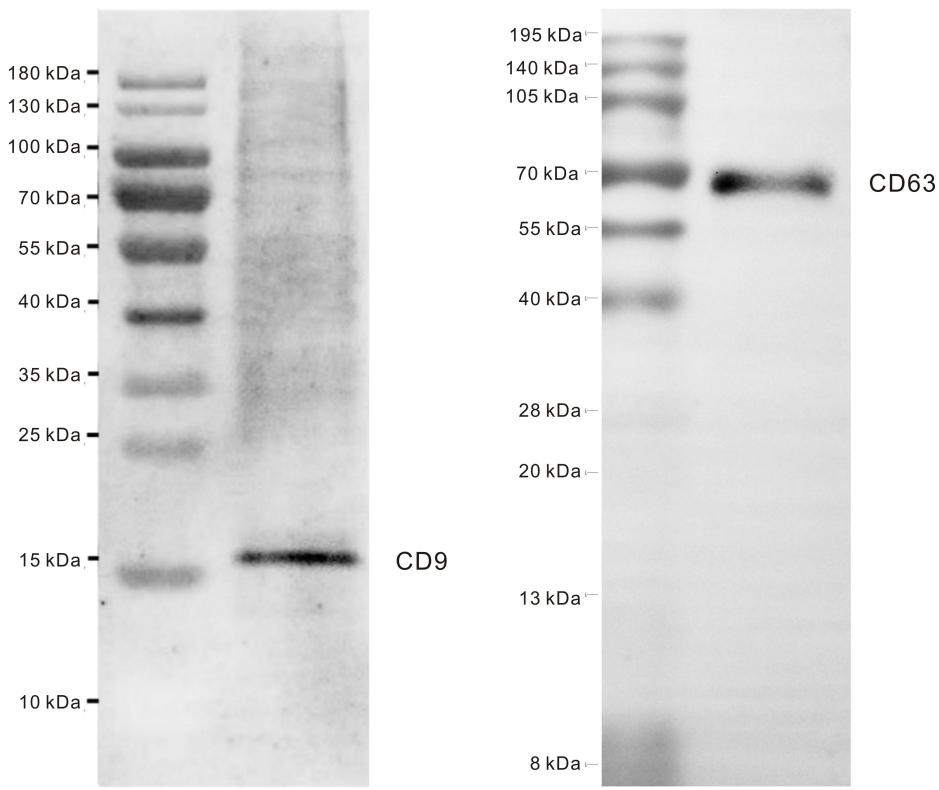

Figure 2 Exosome CD9 and CD63 Western blot results.

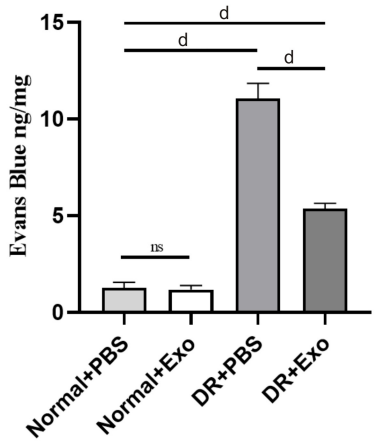

Figure 3 Evans blue results $^{d}P<0.001$, ns: $P>0.05$. Exo: Exosome; PBS: Phosphate buffered saline; DR: Diabetic retinopathy.

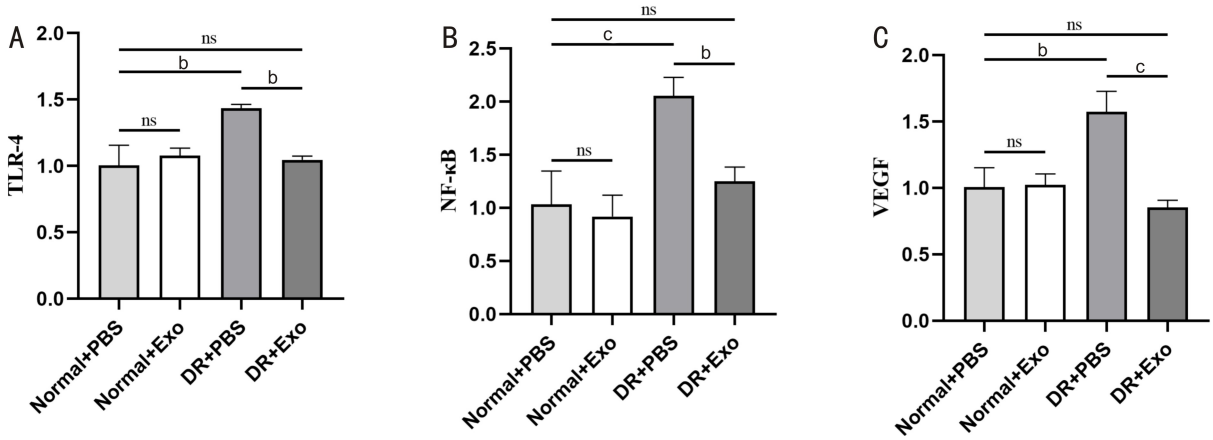

Figure 4 qPCR detection of the mRNA expression of TLR-4, NF-κB and VEGF in the retinas of each group. A: TLR-4 detection results; B: NF-κB detection results; C: VEGF detection results. $^{b}P<0.01$; $^{c}P<0.001$; ns: $P>0.05$. Exo: Exosome; PBS: Phosphate buffered saline; DR: Diabetic retinopathy; TLR-4: Toll-like receptor 4; NF-κB: Nuclear factor kappa-B; VEGF: Vascular endothelial growth factor; qPCR: Quantitative polymerase chain reaction.

BMSC-Exos on Oxidative Stress in the Retinas of DR Rats HE staining indicated that at the 16th week post-modeling, no significant morphological or structural abnormalities were observed in the retinas of Groups A and B. However, Group C exhibited a reduction in the quantity of retinal ganglion cells, a diminished outer plexiform layer, and a disrupted organization of both the inner and outer granular layers (Figure 5A). The immunohistochemistry results indicated that the retinas of Groups A and B were essentially unstained. In comparison, the brownish-yellow staining of the retinal tissue was more pronounced in Group C rats. Following the BMSC-Exo intervention, Group D exhibited a significant decrease in brownish-yellow staining of the retinal tissue (Figure 5B). SOD and GSH are antioxidant enzymes and molecules involved in oxidative stress injury. In our study, ELISA results revealed a significant reduction in brownish-yellow staining of the retinal tissue in Group D compared to the normal group. SOD activity and GSH content were significantly lower in the DR group than in the BMSC-Exo intervention group ($P<0.05$, Figure 6).

BMSC-Exos on Retinal Inflammation in DR Rats Eight weeks following the vitreous injection, ELISA results from rat retinal tissues indicated that the concentrations of IL-6 and TNF-α in the retinal tissues of Groups C and D were markedly higher than those in the retinal tissues of Groups A and B ($P<0.001$). Additionally, the levels of IL-6 and TNF-α in Group D were significantly reduced after treatment with BMSC-Exos ($P<0.01$, Figure 7).

BMSC-Exos on Retinal Cell Apoptosis in DR Rats The TUNEL staining results for each group indicated that the retinas of Groups A and B remained largely unstained, suggesting that BMSC-Exos did not influence the apoptosis of normal retinal tissues. In contrast, the retinal tissue in Group C exhibited a more pronounced red color, suggesting a significant increase in the degree of retinal cell apoptosis in DR rats, particularly evident in the ganglion cell layer and the outer nuclear layer. Following intervention with BMSC-Exos, the number of apoptotic cells in Group D was notably reduced (Figure 8). The immunofluorescence results indicated that the Iba-1-labeled microglia in Groups A and B were predominantly distributed in the inner and outer plexiform layers. In comparison, the immunofluorescence intensity of the retinal tissues in Group C was notably lower, while the intensity in group D was significantly higher following the intravitreal injection of BMSC-Exos (Figure 9).

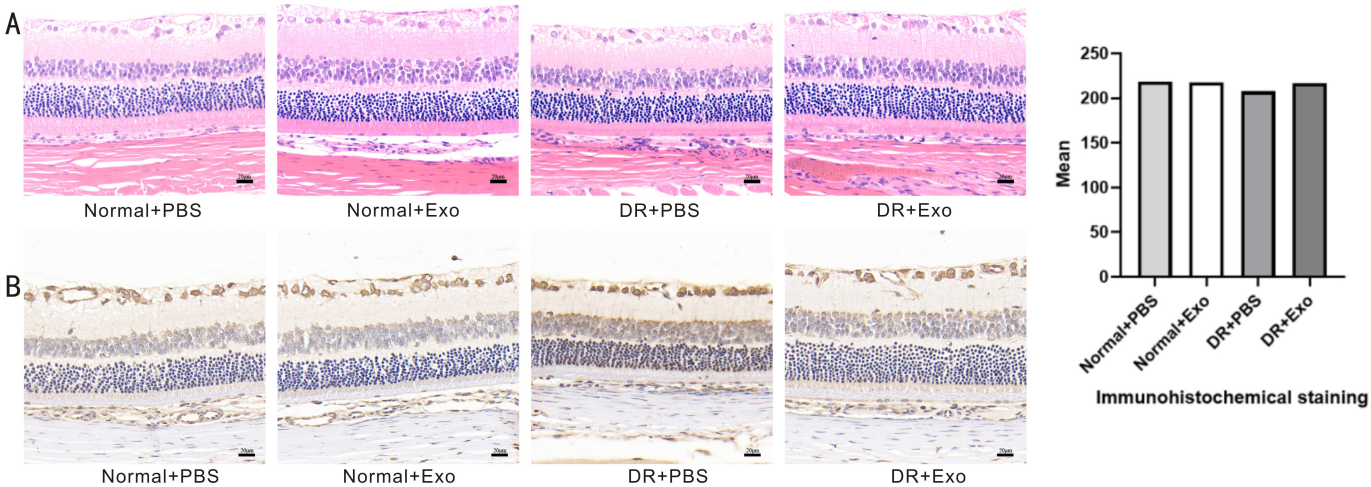

Figure 5 HE staining andimmunohistochemical staining of retinal tissue sections, and the quantification of cell count A: HE staining of retinal tissue from 16-week DR rats (×200); B: Immunohistochemical staining to measure the level of 8-OHdG in the retinal tissue of 16-week DR rats (positively expressed in brownish yellow, ×200). Exo: Exosome; PBS: Phosphate buffered saline; DR: Diabetic retinopathy; HE: Hematoxylin and eosin.

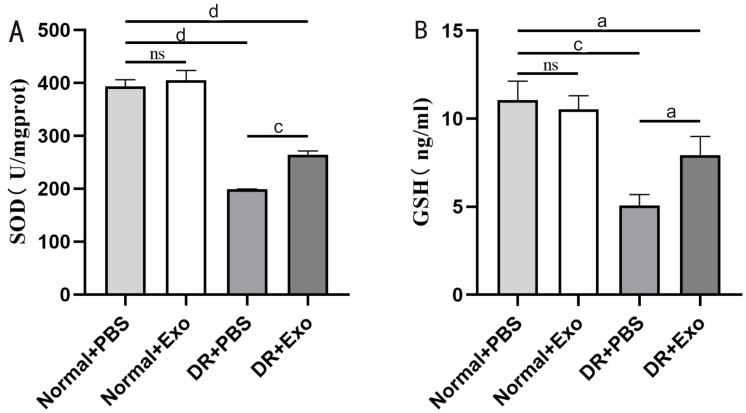

Figure 6 Expression of retinal oxidative stress-related factors A: SOD activity was measured in the retinal tissues of the rats in each group; B: GSH content was measured in the retinal tissues of the rats in each group. $^{a}P<0.05$, $^{c}P<0.001$, $^{d}P<0.0001$, ns: $P>0.05$. Exo: Exosome; PBS: Phosphate buffered saline; DR: Diabetic retinopathy; SOD: Superoxide dismutase; GSH: Glutathione.

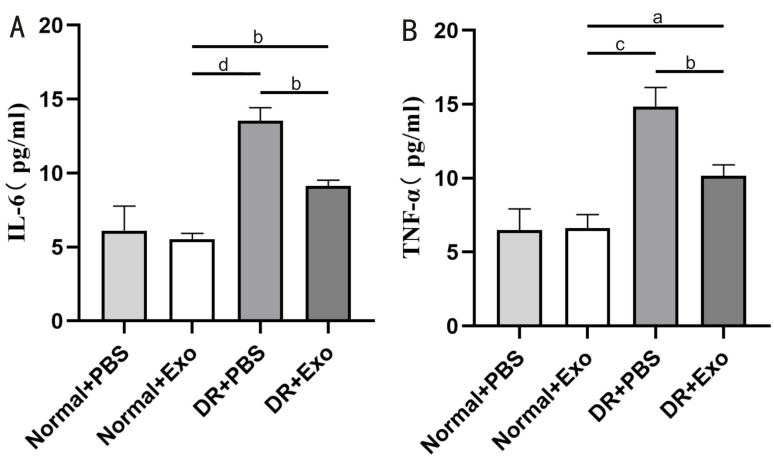

Figure 7 Expression of retinal inflammatory factors A: Measurement of the IL-6 content in the retinal tissues of the rats in each group; B: Measurement of the TNF-α content in the retinal tissues of the rats in each group. $^{a}P<0.05$, $^{b}P<0.01$, $^{c}P<0.001$, $^{d}P<0.001$. Exo: Exosome; PBS: Phosphate buffered saline; DR: Diabetic retinopathy; IL: Interleukin; TNF-α: Tumor necrosis factor-alpha.

DISCUSSION

Diabetes mellitus is a condition that is becoming increasingly prevalent globally. Approximately one-third of patients with diabetes have varying degrees of retinopathy, which can seriously threaten their visual acuity if not treated promptly[8]. Oxidative stress, induced by high glucose levels, is closely associated with early retinal damage and neovascularization in the diabetic retina. Elevated glucose triggers the production of

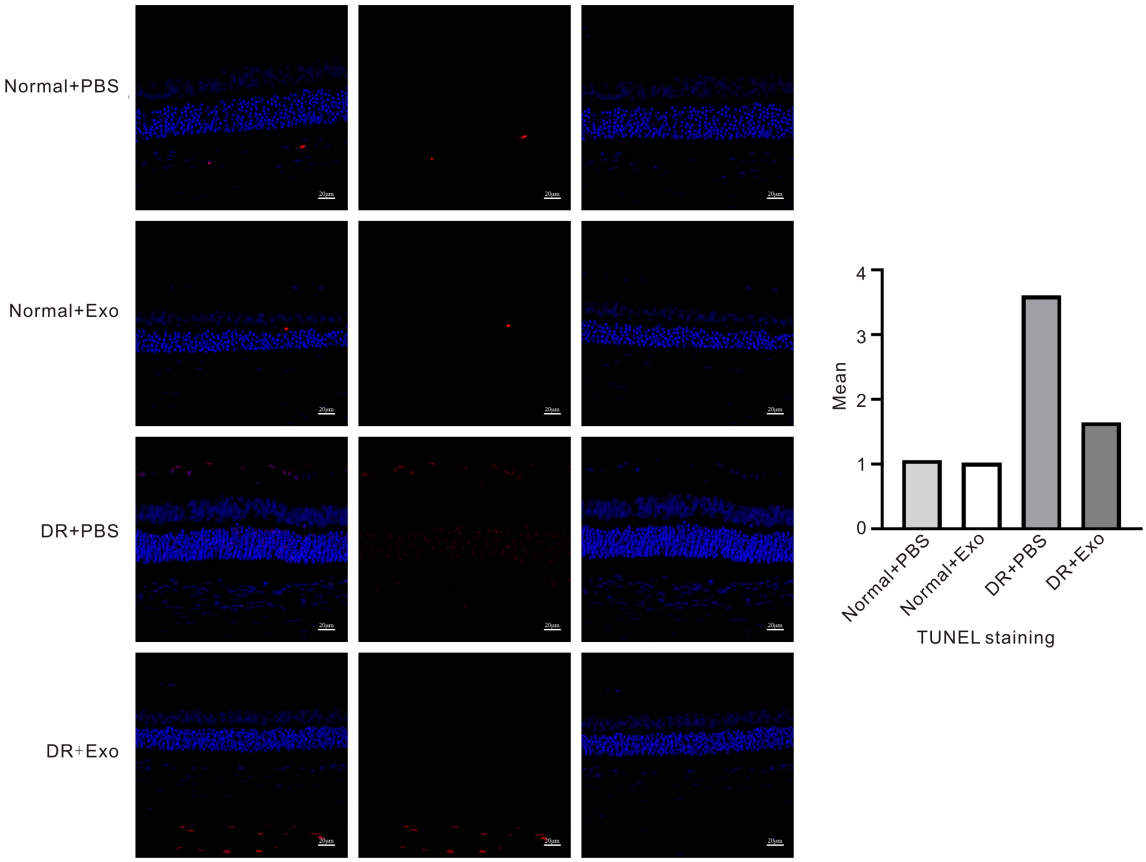

Figure 8 TUNEL staining of retinal tissues from each group, and the quantification of cell count The number of apoptotic cells in Group D (DR+Exo) was notably reduced (positive expression in red, ×200). TUNEL: Terminal deoxynucleotidyl transferase dUTP Nick End Labeling; Exo: Exosome; PBS: Phosphate buffered saline; DR: Diabetic retinopathy.

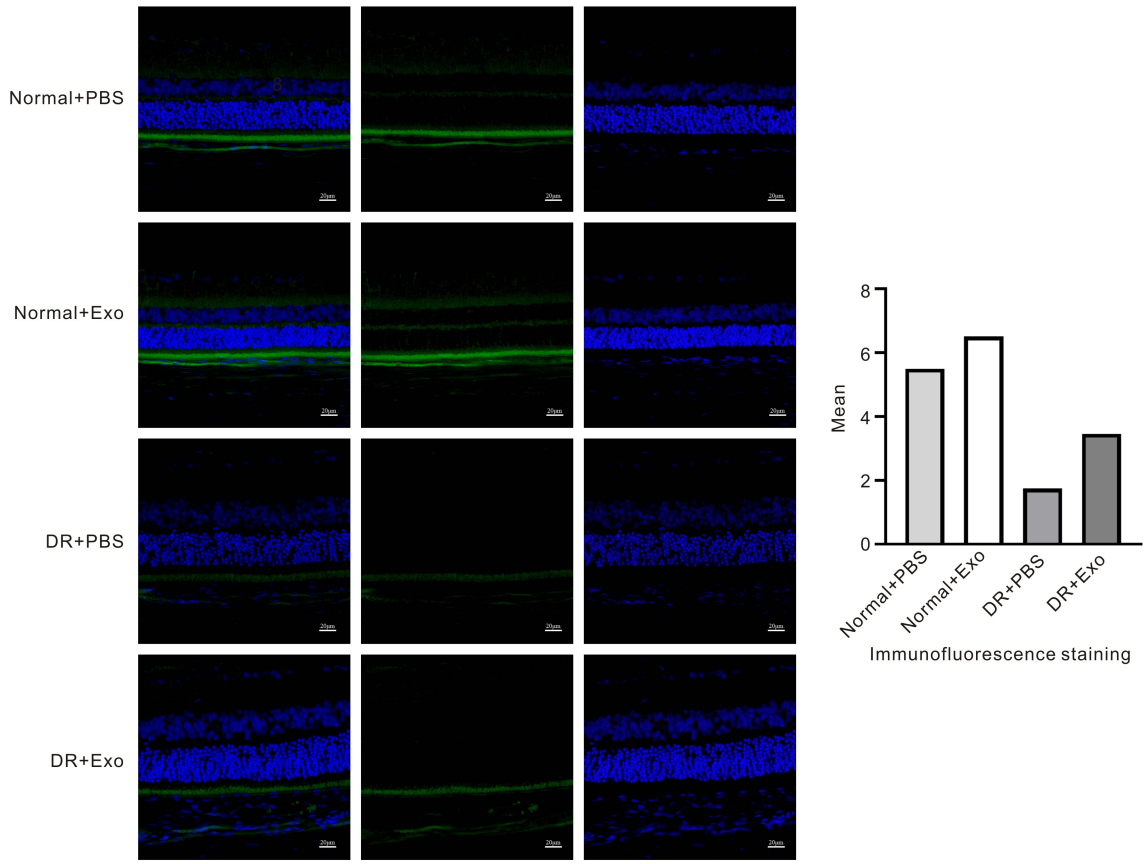

Figure 9 Immunofluorescence staining of retinas from each group, and the quantification of cell count The retinal tissues in Group C (DR+PBS) was notably lower, while the intensity in Group D (DR+Exo) was significantly higher (positive expression is shown in green, ×200). Exo: Exosome; PBS: Phosphate buffered saline; DR: Diabetic retinopathy.

ROS, which in turn activate several oxidative stress-related signaling pathways, including the protein kinase C (PKC) and TLR4/NF-κB pathways. This activation ultimately leads to apoptosis, tissue damage, insulin resistance, and various other complications[9]. Recent research on DR has focused on oxidative stress, inflammation, and VEGF production[10]. In a high-glucose state, the TLR4/NF-κB signaling pathway crucially mediates cellular inflammation and oxidative stress. The expression of TLR4 in the retina is elevated in this condition, activating various pathways that contribute to DR[11]. Downstream NF-κB dimers can enter the nucleus and regulate the expression of corresponding target molecules, thereby inducing inflammatory responses[12].

In DR model mice induced with STZ, the TLR4/NF-κB pathway was significantly stimulated, leading to the release of inflammatory cytokines. Additionally, the expression of glial fibrillary acidic protein (GFAP) and VEGF was also significantly increased[13]. Moreover, cellular experiments have shown that under high-glucose conditions, the expression of TLR4 is increased in retinal ganglion cells[14], under conditions of high hyperglycemia, suppression of TLR4 reduces apoptosis and inflammation in retinal ganglion cells. This suggests that the TLR4/NF-κB signaling pathway could be a potential target for the treatment of DR[15]. DR therapy has advanced significantly as a result of numerous studies that focus on the TLR4/NF-κB signaling pathway. For instance, microRNA-27a can reduce TLR4 and inflammation-related expression, thereby protecting retinal pigment epithelial cells in high-glucose environments[16]. miR-486-3p inhibits TLR4/NF-κB expression, reduces oxidative damage and inflammation, and promotes Müller cell proliferation to decelerate the progression of DR[17]. Our findings are consistent with those of other studies, indicating that the outer nuclear layer of the retina is thinner in rats with DR compared to normal rats[18]. Furthermore, the TLR4/NF-κB signaling pathway, inflammatory release, and VEGF expression were significantly elevated. Immunohistochemical analysis revealed a notable increase in retinal oxidative stress, accompanied by a reduction in the activity of the antioxidant factor SOD and a decrease in the content of GSH content.

Exosomes derived from MSCs are efficient drug carriers *in vivo* and have been demonstrated to prevent oxidative stress and repair various organ and tissue damages, including those affecting the heart, liver, lungs, kidneys, and neurons[19]. In this study, the expression of TLR4, NF-κB, and VEGF was found to be lower in DR rats following intervention with BMSC-Exo compared to those in the nonintervention group. Additionally, the expression levels of inflammatory factors, such as IL-6 and TNF-α, were significantly decreased following intervention with BMSC-Exos. Retinal oxidative stress was reduced, and the activity of SOD and the content of GSH significantly increased. Furthermore, retinal cell apoptosis was markedly diminished after treatment with BMSC-Exos, as evidenced by TUNEL staining. TNF-α is a small protein molecule secreted by macrophages, and its expression is regulated by the NF-κB signaling pathway. On the one hand, IL-6 can directly promote neovascularization; on the other hand, it can also induce neovascularization by promoting the secretion of VEGF[20]. These results indicate that BMSC-Exos can inhibit the TLR4/NF-κB signaling pathway, reduce retinal oxidative stress, attenuate the inflammatory response, and decrease apoptosis. Consequently, they play a protective role in the retina of DR rats.

Microglia are immune cells that exist within the central nervous system. In normal retinal tissues, they function as macrophages and maintain retinal synaptic function, ensuring normal visual function[21]. Microglia are activated at an early stage in DR rat retina; however, a high-glucose environment also induces microglial pyroptosis *via* pathways such as NLRP3 inflammatory vesicles[22], whereas BMSC-Exos are capable of reducing microglial pyroptosis *in vivo*[23]. Studies focusing on microglia have revealed that microglial activation can assume various roles *via* two distinct phenotypes: M1 and M2. When the M1 phenotype is present, pro-inflammatory factors like TNF-α, IL-1β, and IL-6 are released, whereas theM2 phenotype leads to the release of anti-inflammatory factors such as IL-4, IL-10, and TGF-β[24]. Inhibiting the polarization of M1 or promoting the conversion of M1 polarization to M2 polarization can play a role in treating this disease[25]. BMSC-Exos can modulate the transformation of microglia from the M1 phenotype to the M2 phenotype, thus mitigating neuroinflammation and cellular pyroptosis triggered by cerebral ischemia-reperfusion injury[26]. In the treatment of DR, the TLR4/MyD88/NF-κB p65 signaling pathway can be utilized to inhibit microglial M1 polarization and induce M2 polarization, thereby improving early-stage DR[27]. Our study revealed that Iba-1 expression decreased in the DR group at week 16 and increased following the injection of BMSC-Exo. These findings suggest that BMSC-Exos may reduce microglial pyroptosis in the retina of DR rats and improve the progression of DR by promoting microglial M2 polarization; however, further experimental studies are required.

In summary, the administration of BMSC-Exos into the vitreous of DR rats suppressed the TLR4/NF-κB signaling pathway and enhanced retinal oxidative stress, inflammatory release, and apoptosis. This treatment could prove valuable in the early stages of DR. Additionally, BMSC-Exos ameliorated microglial pyroptosis and may promote microglial M2 polarization to retard DR progression *via* the TLR4/NF-κB signaling pathway, though further experimental studies are required.

Conflicts of Interest: Wang Q, None; Zeng F, None; Liu W, None; Huang H, None; Wang HZ, None.

REFERENCES

[1] Altmann C, Schmidt MHH. The role of microglia in diabetic retinopathy: inflammation, microvasculature defects and neurodegeneration. Int J Mol Sci, 2018,19(1):110.

[2] Wei LD, Sun X, Fan CX, et al. The pathophysiological mechanisms underlying diabetic retinopathy. Front Cell Dev Biol, 2022,10:963615.

[3] Kim JJ, Sears DD. TLR4 and insulin resistance. Gastroenterol Res Pract, 2010,2010:212563.
[4] Kawasaki T, Kawai T. Toll-like receptor signaling pathways. Front Immunol, 2014,5:461.
[5] Morgan MJ, Liu ZG. Crosstalk of reactive oxygen species and NF-κB signaling. Cell Res, 2011,21(1):103-115.
[6] Hui Y, Yin Y. microRNA-145 attenuates high glucose-induced oxidative stress and inflammation in retinal endothelial cells through regulating TLR4/NF-κB signaling. Life Sci, 2018,207:212-218.
[7] Xiong JC, Hu H, Guo R, et al. Mesenchymal stem cell exosomes as a new strategy for the treatment of diabetes complications. Front Endocrinol, 2021,12:646233.
[8] Chen XD, Gardner TW. A critical review: psychophysical assessments of diabetic retinopathy. Surv Ophthalmol, 2021,66(2):213-230.
[9] Singh A, Kukreti R, Saso L, et al. Mechanistic insight into oxidative stress-triggered signaling pathways and type 2 diabetes. Molecules, 2022,27(3):950.
[10] Rodríguez ML, Pérez S, Mena-Mollá S, et al. Oxidative stress and microvascular alterations in diabetic retinopathy: future therapies. Oxid Med Cell Longev, 2019,2019:4940825.
[11] Bayan N, Yazdanpanah N, Rezaei N. Role of toll-like receptor 4 in diabetic retinopathy. Pharmacol Res, 2022,175:105960.
[12] Yuan SH, Liu HX, Yuan D, et al. PNPLA3 I148M mediates the regulatory effect of NF-κB on inflammation in PA-treated HepG2 cells. J Cell Mol Med, 2020,24(2):1541-1552.
[13] Fu HY, Liu HQ. Deletion of toll-like receptor 4 ameliorates diabetic retinopathy in mice. Arch Physiol Biochem, 2023,129(2):519-525.
[14] Zhao M, Li CH, Liu YL. Toll-like receptor (TLR)-2/4 expression in retinal ganglion cells in a high-glucose environment and its implications. Genet Mol Res, 2016,15(2):gmr.15026998.
[15] Hu LL, Yang HX, Ai M, et al. Inhibition of TLR4 alleviates the inflammation and apoptosis of retinal ganglion cells in high glucose. Graefes Arch Clin Exp Ophthalmol, 2017,255(11):2199-2210.
[16] Tang XL, Dai Y, Wang XL, et al. microRNA-27a protects retinal pigment epithelial cells under high glucose conditions by targeting TLR4. Exp Ther Med, 2018,16(1):452-458.
[17] Li W, Jin L, Cui Y, et al. Bone marrow mesenchymal stem cells-induced exosomal microRNA-486-3p protects against diabetic retinopathy through TLR4/NF-κB axis repression. J Endocrinol Invest, 2021,44(6):1193-1207.
[18] Zhang Q, Xiao XH, Zheng J, et al. Compound Danshen dripping pill inhibits retina cell apoptosis in diabetic rats. Front Physiol, 2018,9:1501.
[19] Zhang WW, Wang TY, Xue YY, et al. Research progress of extracellular vesicles and exosomes derived from mesenchymal stem cells in the treatment of oxidative stress-related diseases. Front Immunol, 2023,14:1238789.
[20] Staszewski J, Skrobowska E, Piusińska-Macoch R, et al. IL-1α and IL-6 predict vascular events or death in patients with cerebral small vessel disease-data from the SHEF-CSVD study. Adv Med Sci, 2019,64(2):258-266.
[21] Wang X, Zhao L, Zhang J, et al. Requirement for microglia for the maintenance of synaptic function and integrity in the mature retina. J Neurosci, 2016,36(9):2827-2842.
[22] Huang LB, You JM, Yao Y, et al. High glucose induces pyroptosis of retinal microglia through NLPR3 inflammasome signaling. Arq Bras Oftalmol, 2021,84(1):67-73.
[23] Wang JQ, Sun HH, Guo RY, et al. Exosomal miR-23b-3p from bone mesenchymal stem cells alleviates experimental autoimmune encephalomyelitis by inhibiting microglial pyroptosis. Exp Neurol, 2023,363:114374.
[24] Ban ML, Su H, Zeng XB, et al. An active fraction from Spatholobus suberectus dunn inhibits the inflammatory response by regulating microglia activation, switching microglia polarization from M1 to M2 and suppressing the TLR4/MyD88/NF-κB pathway in LPS-stimulated BV2 cells. Heliyon, 2023,9(4):e14979.
[25] Yao YJ, Li JJ, Zhou YF, et al. Macrophage/microglia polarization for the treatment of diabetic retinopathy. Front Endocrinol, 2023,14:1276225.
[26] Liu XL, Zhang MM, Liu HN, et al. Bone marrow mesenchymal stem cell-derived exosomes attenuate cerebral ischemia-reperfusion injury-induced neuroinflammation and pyroptosis by modulating microglia M1/M2 phenotypes. Exp Neurol, 2021,341:113700.
[27] Fang MY, Wan WC, Li QM, et al. Asiatic acid attenuates diabetic retinopathy through TLR4/MyD88/NF-κB p65 mediated modulation of microglia polarization. Life Sci, 2021,277:119567.